Increased functional connectivity of thalamic subdivisions in patients with Parkinson's disease

Conor Owens-Walton[1,*], David Jakabek[2], Brian D. Power[3, 4], Mark Walterfang[5,6], Dennis Velakoulis[5], Danielle van Westen[7, 8, ¶], Jeffrey C.L. Looi[1, 5, ¶], Marnie Shaw[9, ¶] and Oskar Hansson[10, 11, ¶]

[1] Research Centre for the Neurosciences of Ageing, Academic Unit of Psychiatry and Addiction Medicine, School of Clinical Medicine, Medical School, Australian National University, Canberra, Australia

[2] Graduate School of Medicine, University of Wollongong, Wollongong, Australia.

[3] School of Medicine, The University of Notre Dame, Fremantle, Australia

[4] Clinical Research Centre, North Metropolitan Health Service – Mental Health, Perth, Australia

[5] Neuropsychiatry Unit, Royal Melbourne Hospital, Melbourne Neuropsychiatry Centre, University of Melbourne & Northwestern Mental Health, Melbourne, Australia

[6] Florey Institute of Neurosciences and Mental Health, University of Melbourne, Melbourne, Australia

[7] Center for Medical Imaging and Physiology, Skåne University Hospital, Lund, Sweden

[8] Diagnostic Radiology, Department of Clinical Sciences, Lund University, Lund, Sweden

[9] College of Engineering and Computer Science, The Australian National University, Canberra, Australia

[10] Memory Clinic, Skåne University Hospital, Malmö, Sweden

[11] Department of Clinical Sciences, Lund University, Malmö, Sweden

* Corresponding author: conor.owens-walton@anu.edu.au (CO-W)

[¶] Joint senior authors

Abstract

Parkinson's disease (PD) affects 2-3% of the population over the age of 65 with loss of dopaminergic neurons in the substantia nigra impacting the functioning of basal ganglia-thalamocortical circuits. The precise role played by the thalamus is unknown, despite its critical role in the functioning of the cerebral cortex, and the abnormal neuronal activity of the structure in PD. Our objective was to more clearly elucidate how functional connectivity and morphology of the thalamus are impacted in PD (n = 32) compared to Controls (n = 20). To investigate functional connectivity of the thalamus we subdivided the structure into two important regions-of-interest, the first with putative connections to the motor cortices and the second with putative connections to prefrontal cortices. We then investigated potential differences in the size and shape of the thalamus in PD, and how morphology and functional connectivity relate to clinical variables. Our data demonstrate that PD is associated with increases in functional connectivity between motor subdivisions of the thalamus and the supplementary motor area, and between prefrontal thalamic subdivisions and nuclei of the basal ganglia, anterior and dorsolateral prefrontal cortices, as well as the anterior and paracingulate gyri. These results suggest that PD is associated with increased functional connectivity of subdivisions of the thalamus which may be indicative alterations to basal ganglia-thalamocortical circuitry.

Introduction

Parkinson's disease (PD) is the second most common neurodegenerative disorder in the world, affecting 2-3% of the population over the age of 65 [1]. Characteristic motor symptoms of the disorder include resting tremor, rigidity and postural instability. These are accompanied by non-motor symptoms including cognitive impairment, autonomic dysfunction, disorders of sleep-wake cycle regulation, sensory disturbances and pain [2]. The neuropathological hallmark of PD is the presence of α-synuclein-immunopositive Lewy bodies and neurites [3]. This neuropathology results in a degeneration of nigrostriatal dopaminergic neurons, depletion of dopamine across the striatum [4] and consequent dysfunction of basal ganglia-thalamocortical networks [5, 6]. α-synuclein is thought to spread from brainstem regions along the neuraxis, impacting areas of the neocortex at advanced stages of the disease [7]. Dysfunction of basal ganglia-thalamocortical circuits is thus critical as these circuits work in concert with the cortex to mediate a range of cognitive, motor and limbic functions in the brain [8].

To understand the functioning of a network, it is necessary to study the elements of the network and also their interconnections [9]. Investigating elements of brain networks can be done via studying the morphology of key neuroanatomical nuclei acting as 'hubs' within these networks [10]. Hubs are nodes within brain networks that make strong contributions to global network function [11] and the interconnections between these hubs can be investigated through the use of resting-state functional connectivity MRI methods that measure the functioning of intrinsic connectivity networks in the brain at rest [12]. Spontaneous fluctuations of the blood oxygen level-dependent (BOLD) signal that are temporally coherent indicate areas in the brain that may be functionally and anatomically related [13].

As dopamine replacement therapies provide some relief of motor symptoms in PD, significant research effort has focused on the role played by dopaminergic-depleted nuclei of the striatum [14]. However, there is now considerable evidence that the pathology underlying PD affects certain nuclei in the thalamus, and that the structure plays an important role in PD as loss of dopaminergic input to the striatum results in increased GABA-mediated inhibition of thalamocortical projections [15]. The thalamus, considered an integrative hub within functional brain networks [16], is thus an important neuroanatomical structure which we can use to investigate how basal ganglia-thalamocortical circuits are affected in PD, potentially revealing important information about the pathophysiology of the disease.

Functional connectivity (FC) studies implicating the thalamus have yielded inconsistent results with research demonstrating both increased coupling between the thalamus and sensorimotor regions in PD [17] and no significant differences in thalamic FC in PD [18]. Studies have indicated that PD is associated with thalamic volumetric changes compared to control groups [19, 20], while other work presents conflicting data [21-27]. Research has demonstrated subtle morphological changes in a PD cohort compared to controls [19, 23] while other research has found no significant localized shape changes [21, 24, 26]. Although the thalamus plays a key modulatory role in the brain, there is a lack of evidence for a relationship between thalamus volumes and clinical function [21, 22, 27, 28]. Further, there is still significant information to be derived about the precise contribution of component nuclei of the structure, which are impacted differently by the pathological changes that take place in PD. We thus aimed to investigate the FC of relevant functional subdivisions within the thalamus that are crucial in mediating cognitive and motor function. We then sought to investigate possible localized structural changes to the thalamus using a morphological surface-based and volumetric analyses.

We hypothesized that there would be morphological alterations to the thalamus in PD based on the potential impact of PD neuropathology, which has been shown to display neurodegeneration post-mortem [29]. We also hypothesized that there would be a correlation between smaller overall volumes of the thalamus and poorer performance on measures of motor and cognitive function. Finally, we hypothesized that FC of important motor and prefrontal subdivisions of the thalamus would be impacted in PD due to the effect of PD disease processes on basal ganglia-thalamocortical circuits.

Materials and methods

Participants

Participants in this research were members of the Swedish BioFINDER Study (www.biofinder.se). The study is based in Sweden and is affiliated with the Clinical Memory Research Unit and The Biomedical Centre, both at Lund University. Participants were recruited from the Memory and neurology clinics at Skåne University Hospital as well as the Memory Clinic at Ängelholm Hospital. Participants gave written informed consent and this research was performed in accordance with the World Medical Association's Declaration of Helsinki. Participants in the current study received their clinical assessments between 23/05/2012 and 13/03/2014. Ethical approval was obtained through the Ethical Review Board of Lund, Sweden, and the Human Research Ethics Committee at the Australian National University, Canberra, Australia. Diagnosis of PD (n = 32) was made by a neurologist using the National Institute of Neurological and Stroke Diagnostic criteria [30]. A healthy control group (Controls) (n = 20) was used for comparison. Exclusion criteria for the Swedish BioFINDER study included poor knowledge of the Swedish language, developmental

disability, psychiatric disorder, alcohol or substance abuse, the presence of a metabolic disorder, diagnosis of probable PD dementia [31]. A preliminary investigation of functional MRI data indicated a significant difference in subject head motion during image acquisition. We therefore implemented a strict study-specific head motion exclusion criterion of > 0.26mm (defined as mean relative displacement) and used advanced denoising procedures (FSL-FIX) as nuisance regression can be insufficient in removing the spurious effects of movement artifacts in MRI data [32].

All participants underwent a cognitive and neurological examination by a medical doctor with extensive experience in movement disorders. PD patients remained on medication as per their usual regime for both MRI acquisition and clinical assessment, with a levodopa equivalent dosage (LED) metric recorded for each participant. Functioning of participants was quantified with the Unified Parkinson's Disease Rating Scale Part-III test (UPDRS-III), assessing the motor signs of PD [33], the Mini Mental State Examination (MMSE), assessing cognitive mental state [34], the Timed Up and Go test (TUG), assessing mobility [35], the A Quick Test of Cognitive Speed test assessing perception and cognitive speed (AQT) [36] and the Animal Fluency test (AF), assessing verbal fluency and executive function [37].

MRI acquisition

Magnetic resonance imaging was performed on a 3T scanner (Trio, Siemens Magnetom, Erlangen, Germany) equipped with a 20-channel head-coil. High-resolution T1-weighted three-dimensional anatomical brain images were acquired using a magnetization-prepared rapid acquisition technique with gradient-echo sequence (repetition time = 7 ms; echo time = 3 ms; flip angle = 90 degrees; voxel size = isotropic 1=mm^3). Image matrix size was 356 voxels in the coronal and sagittal planes and 176 voxels in the axial plane. Resting state

functional magnetic resonance images (rs-fMRI) (256 volumes per subject) were acquired using T2*-weighted echo planar imaging volumes (repetition time = 1850 ms; echo time 30 ms; flip angle = 90 degrees; matrix 64 × 64; voxel size 3 × 3 × 3.75 mm^3). Image matrix size was 64 voxels in the coronal and sagittal planes and 36 voxels in the axial plane. Subjects were instructed to lie still with their eyes closed, not to fall asleep and not to think of anything in particular during the scan, which lasted for approximately 8 minutes.

Manual segmentation of the thalamus

Manual region-of-interest tracing was performed on participant's T1 MRI data, using ANALYZE 12.0 software (Mayo Biomedical Imaging Resource, Rochester, Minnesota, USA) following a validated method [38]. The tracing for each thalamus was saved as a binary image for rs-fMRI seed-based FC and shape-based morphological analyses. A detailed explanation of the manual tracing method and associated reliability statistics is available in Supplementary Information '*Manual segmentation of the thalamus.*'

Resting-state fMRI preprocessing

All rs-fMRI preprocessing used FMRIB Software Library (FSL) software package tools (FMRIB Software Library, Oxford, UK; FSL version 5.0.10, RRID:SCR_002823) [39]. FMRI Expert Analysis Tool (FEAT) (version 6.00) was used for the removal of the first 6 volumes, motion correction using FMRIB Motion Correction Linear Registration Tool (MCFLIRT) [40], slice-timing correction using Fourier-space timeseries phase-shifting, removal of non-brain structures using FSL's Brain Extraction Tool (BET) [41], spatial smoothing using a full-width half-maximum gaussian kernel of 5 mm, grand mean intensity normalization and high-pass temporal filtering (gaussian-weighted least-squares straight line fitting, with sigma = 50.0s) [42]. Registration of functional images to subjects structural

188 images used boundary-based registration [43] within the FMRIB Linear Registration Tool
189 (FLIRT) [40, 44]. Registration of functional images to Montreal Neurological Institute (MNI)
190 152 T1 2mm^3 standard space was also performed using FLIRT with 12 degrees of freedom,
191 further refined using FNIRT nonlinear registration [45, 46] with a warp resolution of 10mm
192 and a resampling resolution of 4mm. Denoising of head motion, scanner and cerebrospinal
193 fluid artefacts was performed using a probabilistic Multivariate Exploratory Linear
194 Optimized Decomposition into Independent Components (MELODIC version 3.15)
195 independent component analysis method [47]. FSL's ICA-based Xnoiseifier (FIX version
196 1.06) [48] was then used to classify components as either signal or noise, with noise
197 components and also motion confounds (24 regressors) regressed from the data. For the full
198 explanation of the denoising procedure see Supplementary Information '*Independent*
199 *component analysis denoising.*'
200
201 The Oxford Thalamic Structural Connectivity Probability Atlas [49] within FSL's
202 visualization GUI FSLeyes was used to parcellate bilateral thalamic manual segmentation
203 masks into two seed regions-of-interest masks (seed-ROIs) (Fig 1), representing important
204 functional subdivisions of the thalamus. Due to the cardinal motor symptoms in PD, our first
205 seed-ROI incorporated voxels with the highest probability of connectivity with pre- and
206 primary motor cortices and are intended to represent the ventral lateral posterior, ventral
207 lateral and ventral anterior thalamic nuclei. Due to the significant cognitive dysfunction
208 observed in PD, our second seed-ROI incorporated voxels with the highest probability of
209 connectivity to the prefrontal cortex, intended to represent the mediodorsal and anterior
210 thalamic nuclei [49]. For ease of reference we will refer to these seed-ROIs as the VLp/VA
211 thalamus and MD/A thalamus, respectively. Generic VLp/VA and MD/A thalamic masks
212 were thresholded to only include voxels that had a greater than 50% chance of inclusion, then

registered to subject-specific functional MRI space, and finally eroded by zeroing non-zero voxels when found in kernel, to reduce partial volume effects. A visual inspection of a subset of VLp/VA and MD/A masks was then performed to check the alignment of masks within functional data. We then extracted the mean activation of the functional data within the two seed-ROI masks at each functional timepoint for use as explanatory variables at the individual-level general linear model (GLM) stage in a mass univariate voxelwise whole-brain analysis. The average number of voxels per seed-ROI for each group and a pairwise comparison of this data is shown in Supplementary Information '*Atlas-based ROI segmentation statistics*.'

<Insert Fig 1 here>

Fig 1. Positioning and likelihood-map of seed voxels for VLp/VA and MD/A thalamic masks. This figure displays the voxels used in seed-ROI masks for the functional connectivity analyses, overlaid on MNI T1 0.5mm images. This image was produced by combining all of the binary masks of each participant into one unified mask, with warm (yellow - red) colors indicating the positioning of the VLp/VA voxels and cold colors (light blue - dark blue) indicating the positioning of the MD/A voxels. Darker tones are indicative of a greater proportion of voxels in that region being included in the relevant seed-ROI mask. VLp/VA, ventral lateral posterior and ventral anterior thalamic voxels; MD/A, mediodorsal and anterior thalamic voxels.

Resting-state fMRI statistical analyses

Two individual-level FC analyses were performed for each participant, using a GLM approach [50]. BOLD timeseries data within the VLp/VA and MD/A thalamus were correlated with activity in the rest of the brain, shifting the model with a temporal derivative to account for lags in the onset of the hemodynamic response function, removing volumes corrupted by large motion and regressing out average timeseries data from whole brain (global signal regression), white matter and ventricle masks. For the full explanation of our approach to individual-level GLM analyses, see Supplementary Information '*Individual-level GLM functional connectivity analyses.*' Higher-level analysis of FC differences between PD

and Control subjects were investigated in standard space using FSL-FEAT. We chose a nonparametric permutation-based approach (n = 5000) [51] via FSL-randomise [52] with a threshold-free cluster enhancement method controlling the family-wise error rate at $p < 0.05$. This approach avoids selecting arbitrary threshold values, while also potentially improving sensitivity to test signal shapes and SNR values [53]. Due to there being a significant difference in education between PD and Control groups, we included years of education as a covariate, along with age and sex.

Correlation between functional connectivity and clinical data

To investigate the relationship between FC and clinical variables we conducted a series of post-hoc partial correlational analyses. These focused on the average parameter estimate for VLp/VA and MD/A thalamus at the peak voxel locations derived from the between group analyses. Spherical ROIs (7mm radius) were generated around the voxel locations with the average parameter estimate extracted for each subject. Average FC for each ROI was then correlated against LED, disease duration, UPDRS-III, TUG, AQT and Animal Fluency scores.

Morphology of the thalamus in PD

Volumetric analyses

To investigate differences in volumes of the thalamus between PD and Controls we used SPSS 22.0 (IBM Corporation, Somers, New York, USA) utilizing multivariate analysis of covariance models controlling for estimated total intracranial volume (eTIV, derived from recon-all FreeSurfer processing [54]), age and sex. Effect sizes are represented by partial eta squared values (η^2).

Surface based shape analysis

Shape analysis was performed using spherical harmonic parameterization and sampling in a three-dimensional point distribution model (SPHARM-PDM) [55] outlined in detail in Supplementary Information '*SPHARM-PDM detail.*' Generally speaking, SPHARM-PDM shape analysis provides visualizations of the local surface changes to the thalamus between groups via mean difference displacement maps, mapping the magnitude of surface change (deflation or inflation) in millimeters between corresponding points on the mean surfaces of the PD subjects compared to Controls. Significant surface change was displayed at $p < 0.05$ with a correction for multiple comparisons performed using a false-discovery rate bound q of 5% [56].

Correlations between thalamic volumes and clinical symptoms

We used hierarchical multiple regression models to assess whether thalamic volumes can predict clinical symptoms. These models incorporated two levels, the first level controlled for eTIV, age, sex and years of education (the latter when dealing with measures of cognitive function), and the second level held the independent variable of interest (volume of right or left thalamus), measuring the unique contribution of that variable in predicting each measure of clinical function. Effect sizes are represented by standardized beta values (β).

Results

Participant characteristics

There were no significant differences in age, head size (eTIV) or proportions of males and females in groups, between the PD cohort and Controls. Years of education, UPDRS-III and AQT performance was significantly reduced in PD compared to Controls (Table 1).

Table 1. Demographic and clinical characteristics of participants.

Item	Controls	PD	*p*-value
Number of participants	20	32	-
Female/Male	10/10	18/14	0.878
Age	69.06 ± 6.86	69.36 ± 5.82	0.868
LED	-	523.36 ± 295.31	-
Disease duration	-	5.16 ± 3.62	-
eTIV (cm^3)	156.81 ± 15.84	152.06 ± 17.71	0.333
Years of education	13.14 ± 3.68	9.78 ± 6.05	0.042
Relative displacement	0.13 ± 0.06	0.16 ± 0.06	0.066
H&Y	-	1.75 ± 0.55	-
UPDRS-III	2.40 ± 3.02	10.69 ± 7.06	<0.001
TUG	8.60 ± 1.54	9.68 ± 2.39	0.079
MMSE	28.8 ± 1.2	28.28 ± 1.42	0.18
AQT	57.25 ± 15.09	66.47 ±14.78	0.035
AF	24.80 ± 6.59	23.03 ± 5.67	0.309

Data presented as mean ± standard deviation; *p*-values, one-way independent samples *t*-test, excluding male/female numbers which was analyzed via a chi-square test for independence; LED, levodopa equivalent dosage (mg); eTIV, estimated total intracranial volume; Relative displacement, mean value derived from MCFLIRT FSL motion correction; H&Y, Hoehn and Yahr Scale; UPDRS-III, Unified Parkinson's Disease Rating Scale part III; TUG, Timed Up and Go test; MMSE, Mini Mental-state Examination; AQT, A quick test of cognitive speed; AF, Animal fluency test.

Functional connectivity of the VLp/VA thalamus in PD

Analysis of the VLp/VA thalamus in PD found significant clusters of increased FC with the right supplementary motor area (BA6) and the left paracingulate gyrus (BA32). Analysis of

the VLp/VA thalamus also found a significant cluster of decreased FC with the left lateral occipital cortex (BA19) (Fig 2, Table 2).

<Insert Fig 2>

Fig 2. VLp/VA thalamus functional connectivity. *p*-value images showing neuroanatomical regions with significant between-group changes in functional connectivity with the VLp/VA thalamus in PD subjects compared to Controls. Warm colors (yellow-orange) represent areas of increased functional connectivity in PD and cool colors (light-dark blue) represent areas of decreased functional connectivity in PD. Spacing between each slice in the z-direction is 4.2mm beginning at z = -3.18 in the top left slice (MNI T1 2mm image). R, right; A, anterior; PCG, paracingulate gyrus; SMA, supplementary motor area; LOC, lateral occipital cortex.

Table 2. Regions showing functional connectivity differences with the VLp/VA thalamus in PD.

				MNI		
FC Cluster	**Peak**	**Brain regions**	**Voxels**	**x**	**y**	**z**
Increased	1	R Supplementary motor area (BA6)	64	12	-2	42
	2	L Paracingulate gyrus (BA32)	11	-4	10	42
	3	R Supplementary motor area (BA6)	10	10	6	44
Decreased	4	L Lateral occipital cortex (BA19)	18	-30	-86	24
	5	L Lateral occipital cortex (BA19)	10	-26	-66	46
	6	L Lateral occipital cortex (BA19)	3	-26	-68	56

Brain regions and associated coordinates represent significant peaks within each cluster ($p < 0.05$). Abbreviations: FC, functional connectivity; L, left hemisphere; R, right hemisphere; BA, Brodmann area; MNI, coordinates for location of peak voxels in Montreal Neurological Institute 152 T1 2mm space. Labelling of brain regions based on the Harvard-Oxford Cortical/Subcortical Atlases.

Functional connectivity of the MD/A thalamus in PD

Analysis of the MD/A thalamus in PD found significant clusters of increased FC with the left anterior cingulate (BA24) and left putamen (Fig 3, Table 3). These clusters extended across the following brain regions: the bilateral anterior (BA24) and paracingulate gyri (BA32), left caudate nucleus, left putamen, left globus pallidus, bilateral dorsolateral prefrontal cortex

(BA9) and bilateral anterior prefrontal cortex (BA8). Analysis of the VLp/VA thalamus also found a significant cluster of decreased FC with the left lateral occipital cortex (BA19).

<Insert Fig 3>

Fig 3. MD/A thalamus functional connectivity. *p*-value images showing neuroanatomical regions with significant between-group changes in functional connectivity of the MD/A thalamus in PD subjects compared to Controls. Warm colors (yellow-orange) represent areas of increased functional connectivity in PD. Spacing between each slice in the z-direction is 4mm beginning at z = -2.3 in the top left slice (MNI T1 2mm image). R, right; A, anterior; Put, putamen; GP, globus pallidus; CN, caudate nucleus; PCG, paracingulate gyrus; ACC, anterior cingulate cortex; DLPFC, dorsolateral prefrontal cortex; APFC, anterior prefrontal cortex.

Table 3. Regions showing functional connectivity differences with the MD/A thalamus in PD.

				MNI		
FC Cluster	**Peak**	**Brain regions**	**Voxels**	**x**	**y**	**z**
Increased	7	L anterior cingulate (BA24)	4319	-8	18	22
	8	L putamen (BA49)	268	-20	10	-4
Decreased	9	L lateral occipital cortex (BA19)	10	-18	-78	52

Brain regions and associated coordinates represent significant peaks within each cluster ($p < 0.05$). Abbreviations: FC, functional connectivity; L, left hemisphere; R, right hemisphere; BA, Brodmann area; MNI, coordinates for location of peak voxels in Montreal Neurological Institute 152 T1 2mm space; Labelling of brain regions are based on the Harvard-Oxford Cortical/Subcortical Atlases.

Correlation between functional connectivity and clinical data

In PD patients we observed a positive correlation between LED and mean FC of the right supplementary motor area (peak 3; r = 0.46, $p = 0.01$) and a negative correlation with the left lateral occipital cortex (peak 4; r = -0.41, $p = 0.04$). We also observed a positive correlation between disease duration and mean FC of the right supplementary motor area (peak 1; r = 0.41, $p = 0.03$; peak 3; r = 0.57, $p = 0.01$). We also observed a positive correlation between TUG scores and mean FC of the left paracingulate gyrus (peak 2; r = 0.43, $p = 0.02$) and

lateral occipital cortex (peak 6; r = 0.43, p = 0.02; peak 9; r = 0.37, p = 0.047). None of these results survived correction for multiple comparisons (*Supplementary Information Table S1*).

Morphology of the thalamus in PD

Volumetric analyses

Comparisons of thalamic volumes found no difference between the PD group and Controls (Table 4).

Table 4: Estimated mean volumes of right and left thalamus and pairwise comparison.

Structure	Control	PD	Mean difference	*p*-value
Right thalamus volume (mm^3)	5774.13	5927.45	-153.32	0.25
Left thalamus volume (mm^3)	5594.47	5749.24	-154.78	0.18

Estimated volumes of the right and left thalamus after adjusting for age, eTIV and sex. *p*-value presented has been adjusted for family-wise error rate using a Bonferroni correction.

Surface based shape analysis

Shape analysis found no localized areas of shape change to the surface of the right or left thalamus in the PD group compared to Controls, after correcting for false-discovery rate (Fig 4).

<Insert Fig 4>

Fig 4. Shape analysis of thalamus in PD compared to Controls. Displayed are superior and inferior views of bilateral thalami overlaid on axial MNI T1 0.5mm images. Warmer colors indicate regions of greater inflation in the PD group compared to Controls using point-wise significance tests (p < 0.05, uncorrected). No regions were significant after false-discovery rate correction.

Correlations between thalamic volumes and clinical symptoms in PD

We found no significant relationships between volumes of the right or left thalamus and clinical function in the PD or Control groups (*Supplementary Information Table S2*).

Discussion

The results of this study demonstrate that PD patients on medication have increased FC within motor, dorsolateral and anterior cingulate basal ganglia-thalamocortical circuits. Our data support the findings of a recent meta-analysis showing that PD patients have increased FC of basal ganglia-thalamocortical circuity [57], and extend these findings by showing how important functional subterritories of the thalamus are impacted in PD. These changes in FC were found despite any evidence of morphological alterations to the thalamus.

Our findings of increased FC between the VLp/VA thalamus and the supplementary motor area may be indicative of changes within one segment of the classic 'motor' basal ganglia-thalamocortical circuit [5]. In this model, the motor circuit originates at the supplementary motor area, receiving input from the primary and the premotor cortices. These areas connect with the nuclei of the basal ganglia, which project back to the ventral anterior and ventral lateral nuclei of the thalamus, closing the loop by reconnecting with the site of origin in motor cortical areas [5]. Increased FC between the putamen and the supplementary motor area has been demonstrated previously [58] while other research using graph theoretical analyses has demonstrated increased functional connectivity within the sensorimotor network in PD [59]. Evidence suggests that increased FC of sensorimotor networks is likely related to

391 dopaminergic medication usage [60] potentially facilitating increases in FC, which is a
392 mechanism that will be discussed momentarily.
393
394 Our research also demonstrates significant and far more widespread increases in FC in PD
395 between the MD/A thalamus and the anterior and dorsolateral prefrontal cortices, potentially
396 indicating a disease related change to the 'dorsolateral prefrontal' basal ganglia-
397 thalamocortical circuit [5]. This circuit originates in Brodmann areas 9 and 10 on the lateral
398 surface of the anterior frontal lobe, and after traversing the basal ganglia, connects directly
399 with our intended seed-ROIs at the anterior and mediodorsal nuclei of the thalamus. From
400 there, the circuit projects back to the anterior and dorsolateral prefrontal cortices to form a
401 closed loop [5]. Our findings of increased FC between the MD/A thalamus and the
402 dorsolateral prefrontal cortex may represent functional compensatory mechanisms due to the
403 significant cognitive dysfunction common in PD. The dorsolateral prefrontal cortex helps to
404 execute tasks that contribute to cognitive functioning, including working memory, decision-
405 making and action control, achieved through a top-down modulation of behavior in concert
406 with diverse cortical and subcortical structures [61]. Research has shown that FC is
407 significantly increased *across* the prefrontal cortex in PD subjects on medication, as the brain
408 potentially recruits new anatomical areas to aid in the performance of cognitive tasks. It is
409 argued that changes in FC may indicate a functional compensation to help restore cognitive
410 processes in PD [61]. Interestingly, we also found significant increases in FC between the
411 MD/A thalamus and the anterior cingulate cortex in PD subjects, indicating a disease related
412 change to the 'anterior cingulate' basal ganglia-thalamocortical circuit. In this circuit, the
413 anterior cingulate cortex links with the ventral basal ganglia structures, outputs to the ventral
414 anterior nuclei of the thalamus, and links back with the anterior cingulate cortex [5]. Our
415 findings of increased FC with the anterior as well as paracingulate gyri fit with the concept of

increased FC due to compensatory mechanisms, as this region of the brain interacts with the lateral prefrontal cortex to mediate performance in tasks linked to cognitive processes [62]. Research has shown that a common response to neurological disruption is the *hyper*-connectivity of brain circuits, which may reflect a protective mechanism in the brain to maintain normal functioning [63]. Such a mechanism has been proposed in PD previously [64, 65], as well as in mild cognitive impairment and Alzheimer disease [66, 67], and taken together, our results provide support for this model.

There are nonetheless inconsistencies with similar FC research that require consideration. Our data contrast with work demonstrating no significant FC changes between the thalamus and widescale brain networks in subjects on medication [18]. A possible explanation for this inconsistency may relate to how FC changes across different disease stages. When compared to the current work, the study in question focused on PD subjects with both a longer disease duration as well as a higher average Hoehn and Yahr stage [18]. This is important because research has shown that FC in PD may undergo periods of both *hyper*-connectivity and *hypo*-connectivity as the disease progresses [64]. Potential FC changes across the course of PD thus make difficult to compare studies with subjects at different disease stages.

Our data also indicate that PD is associated with increases in FC between the MD/A thalamus and the left dorsal caudate nuclei, anterior putamen and globus pallidus. Strong evidence suggests that the output of the basal ganglia, mainly the globus pallidus interna, is hyperactive in PD [68] and our results of increased FC with this area suggest that increased activity may be accompanied by increased FC. Increased FC between the caudate nuclei and the thalamus has been shown in a PD cohort on medication [69], however two studies have demonstrated conflicting results [17, 70]. A crucial difference separating these studies relates

441 to patient inclusion. One of these studies focused on early PD patients with a mean disease
442 duration of 1.7 years [17], which differs markedly from the current study where the average
443 disease duration is 5.16 years. The present study also excluded PD subjects with dementia,
444 fundamentally distinguishing it from our previous work [70]. This is crucial as PD dementia
445 is associated with decreases in FC compared to subjects without the diagnosis [71]. Our
446 findings of increased FC between the MD/A thalamus and the anterior putamen are supported
447 by similar research in this field [65]. This research demonstrated that increased inter-regional
448 coupling of the anterior putamen, the region anterior to the anterior commissure, follow the
449 specific spatial pattern of dopamine depletion in PD [4]. This research suggests that PD
450 patients may undergo a shift in cortico-striatal connections from the neuro-chemically more
451 affected posterior putamen toward the relatively spared anterior putamen. Our results support
452 this finding, suggesting that the anterior putamen may undergo increased FC with the MD/A
453 thalamus, further supporting the model that the pathophysiology of PD may involve
454 compensatory alterations in the FC of key nuclei within basal ganglia-thalamocortical
455 circuits.
456
457 While conceiving of FC changes in terms of segregated basal ganglia-thalamocortical circuits
458 is attractive, this inference is theoretical. It is therefore helpful to consider the results of other
459 imaging techniques to substantiate our findings. Graph-based eigenvector centrality mapping
460 research (which informs on the number and quality of node connections within networks) has
461 shown that this metric is increased in the thalamus in PD [72]. Interestingly, we also found a
462 significant (though small) cluster of reduced FC of both the VLp/VA and MD/A thalamus
463 with the lateral occipital cortex in PD patients, supporting previous work which found
464 reductions in FC between nuclei of the extended basal-ganglia (including the thalamus) and
465 this area of the brain [72]. The findings from ^{18}F-flurodeoxyglucose PET imaging has

466 indicated that PD is associated with increased pallidothalamic activity [73], which supports
467 our findings. However, this research also demonstrated that regions of the dorsolateral
468 prefrontal cortex and the supplementary and premotor areas show reductions in metabolic
469 activity in PD, contrasting with our results [73].
470
471 We found no significant correlation between FC of our seed-ROI in the thalamus and
472 measures of clinical function, disease duration or antiparkinsonian medication use. This
473 supports previous meta-analytic research which indicates that FC within a basal-ganglia
474 networks does not correlate with clinical indices of disease severity [74], arguing instead that
475 altered FC reflects a constitutional alteration of the networks under consideration. Our results
476 are also bolstered by meta-analytic findings which indicate that increased FC of the thalamus
477 were unaffected by medication status [57].
478
479 The morphological data from our study are consistent with previous reports indicating that
480 PD is not associated with atrophy of the thalamus [21, 23-28]. We also found no significant
481 localized surface shape changes in the PD group, supporting a number of studies [21, 24, 25].
482 After investigating between-group morphological differences we investigated potential
483 relationships between volumes of the thalamus and measures of clinical function. These
484 analyses revealed no significant findings, supporting previous research [21, 27, 28]. These
485 results make intuitive sense, as we found no significant volumetric or localized shape
486 changes in the PD cohort, suggesting there was no discernable relationship between atrophy
487 of the thalamus and the PD disease process.
488

Strengths and Limitations

Possible limitations of the current work warrant further attention. The first is our small sample size. While this is an important factor that negatively impacts the power of our study, our sample size was the result of choosing a highly stringent head motion exclusion criteria, which we believe is a strength of our work. A second possible limitation is the use of atlas-based seed-ROI segmentation, defined by the structural connectivity of thalamic nuclei [49]. Future work may benefit from a data-driven parcellation scheme as it may better capture functional boundaries of seed-ROIs. Despite these considerations we believe our data make important statements about the role of the thalamus within basal ganglia-thalamocortical circuits in PD.

Conclusions

We found increases in functional connectivity between the VLp/VA thalamus and the supplementary motor area and paracingulate gyrus, and also between the MD/A thalamus and basal ganglia nuclei, anterior and paracingulate cingulate gyri, anterior and also dorsolateral prefrontal cortical regions. Significant increases in functional connectivity were found despite any observable volumetric or localized shape alterations to the thalamus. The results of this study indicate that functional connectivity changes occur in PD, which likely result from disease-related system level dysfunction of the thalamus as a crucial network hub within basal ganglia-thalamocortical circuits.

Acknowledgements

The authors are indebted to all patients and control subjects who participated in this study. This project is an initiative of the Swedish BioFINDER Study, of whom DvW and OH are

steering committee members, and also the AUSSIE network coordinated by JCLL at the Australian National University Medical School, who self-funds related expenses.

Financial disclosure statement

CO-W would like to acknowledge The Australian National University for their funding support via the University Research Scholarship. Work in DvW and OH's laboratory was supported by the European Research Council, the Swedish Research Council, the Strategic Research Area MultiPark (Multidisciplinary Research in Parkinson's disease) at Lund University, the Swedish Brain Foundation, the Parkinson Foundation of Sweden, the Skåne University Hospital Foundation and the Swedish federal government under the ALF agreement. Funding sources had no role in the conduct of this study, its analysis, interpretation of the data or in the preparation, review or approval of the manuscript.

References

1. Poewe W, Seppi K, Tanner CM, Halliday GM, Brundin P, Volkmann J, et al. Parkinson disease. Nature Reviews Disease Primers. 2017;3:17013.
2. Schapira AHV, Chaudhuri KR, Jenner P. Non-motor features of Parkinson disease. Nat Rev Neurosci. 2017;18(7):435-50.
3. Dickson DW, Braak H, Duda JE, Duyckaerts C, Gasser T, Halliday GM, et al. Neuropathological assessment of Parkinson's disease: refining the diagnostic criteria. The Lancet Neurology. 2009;8(12):1150-7.
4. Kish SJ, Shannak K, Hornykiewicz O. Uneven pattern of dopamine loss in the striatum of patients with idiopathic Parkinson's disease. Pathophysiologic and clinical implications. New England Journal of Medicine. 1988;318(14):876-80.
5. Alexander GE, DeLong MR, Strick PL. Parallel organization of functionally segregated circuits linking basal ganglia and cortex. Annual review of neuroscience. 1986;9(1):357-81.
6. DeLong M, Wichmann T. Update on models of basal ganglia function and dysfunction. Parkinsonism & Related Disorders. 2009;15:S237-S40.
7. Braak H, Del Tredici K, Rüb U, de Vos RA, Jansen Steur EN, Braak E. Staging of brain pathology related to sporadic Parkinson’s disease. Neurobiology of Aging. 2003;24(2):197-211.
8. Haber SN. The primate basal ganglia: parallel and integrative networks. Journal of chemical neuroanatomy. 2003;26(4):317-30.

9. Sporns O, Tononi G, Kötter R. The Human Connectome: A Structural Description of the Human Brain. PLoS Computational Biology. 2005;1(4).
10. Sporns O, Honey CJ, Kötter R. Identification and classification of hubs in brain networks. PloS one. 2007;2(10):e1049.
11. van den Heuvel MP, Sporns O. Network hubs in the human brain. Trends in cognitive sciences. 2013;17(12):683-96.
12. Biswal B, Yetkin FZ, Haughton VM, Hyde JS. Functional connectivity in the motor cortex of resting human brain using echo-planar MRI. Magn Reson Med. 1995;34(4):537-41.
13. Fox MD, Raichle ME. Spontaneous fluctuations in brain activity observed with functional magnetic resonance imaging. Nat Rev Neurosci. 2007;8(9):700-11.
14. Caligiore D, Helmich RC, Hallett M, Moustafa AA, Timmermann L, Toni I, et al. Parkinson's disease as a system-level disorder. npj Parkinson's Disease. 2016;2:16025.
15. Obeso JA, Rodríguez‐Oroz MC, Benitez‐Temino B, Blesa FJ, Guridi J, Marin C, et al. Functional organization of the basal ganglia: therapeutic implications for Parkinson's disease. Movement Disorders. 2008;23(S3):S548-S59.
16. Hwang K, Bertolero MA, Liu WB, D'esposito M. The human thalamus is an integrative hub for functional brain networks. Journal of Neuroscience. 2017;37(23):5594-607.
17. Agosta F, Caso F, Stankovic I, Inuggi A, Petrovic I, Svetel M, et al. Cortico-striatal-thalamic network functional connectivity in hemiparkinsonism. Neurobiology of Aging. 2014;35(11):2592-602.
18. Bell PT, Gilat M, O'Callaghan C, Copland DA, Frank MJ, Lewis SJG, et al. Dopaminergic basis for impairments in functional connectivity across subdivisions of the striatum in Parkinson's disease. Human Brain Mapping. 2015;36(4):1278-91.
19. Garg A, Appel-Cresswell S, Popuri K, McKeown MJ, Beg MF. Morphological alterations in the caudate, putamen, pallidum, and thalamus in Parkinson's disease. Frontiers in Neuroscience. 2015;9.
20. Lee S, Kim S, Tae W, Lee S, Choi J, Koh S, et al. Regional volume analysis of the Parkinson disease brain in early disease stage: gray matter, white matter, striatum, and thalamus. American Journal of Neuroradiology. 2011;32(4):682-7.
21. Lee HM, Kwon K-Y, Kim M-J, Jang J-W, Suh S-i, Koh S-B, et al. Subcortical grey matter changes in untreated, early stage Parkinson's disease without dementia. Parkinsonism & related disorders. 2014;20(6):622-6.
22. Mak E, Su L, Williams GB, Firbank MJ, Lawson RA, Yarnall AJ, et al. Baseline and longitudinal grey matter changes in newly diagnosed Parkinson's disease: ICICLE-PD study. Brain. 2015;138(10):2974-86.
23. McKeown MJ, Uthama A, Abugharbieh R, Palmer S, Lewis M, Huang X. Shape (but not volume) changes in the thalami in Parkinson disease. BMC neurology. 2008;8(1):8.
24. Menke RA, Szewczyk‐Krolikowski K, Jbabdi S, Jenkinson M, Talbot K, Mackay CE, et al. Comprehensive morphometry of subcortical grey matter structures in early‐stage Parkinson's disease. Human brain mapping. 2014;35(4):1681-90.
25. Messina D, Cerasa A, Condino F, Arabia G, Novellino F, Nicoletti G, et al. Patterns of brain atrophy in Parkinson's disease, progressive supranuclear palsy and multiple system atrophy. Parkinsonism & related disorders. 2011;17(3):172-6.
26. Nemmi F, Sabatini U, Rascol O, Peran P. Parkinson's disease and local atrophy in subcortical nuclei: insight from shape analysis. Neurobiology of Aging. 2015;36(1):424-33.

27. Tinaz S, Courtney MG, Stern CE. Focal cortical and subcortical atrophy in early Parkinson's disease. Movement Disorders. 2011;26(3):436-41.
28. Mak E, Bergsland N, Dwyer MG, Zivadinov R, Kandiah N. Subcortical atrophy is associated with cognitive impairment in mild Parkinson disease: a combined investigation of volumetric changes, cortical thickness, and vertex-based shape analysis. American Journal of Neuroradiology. 2014;35(12):2257-64.
29. Halliday GM. Thalamic changes in Parkinson's disease. Parkinsonism & Related Disorders. 2009;15, Supplement 3:S152-S5.
30. Gelb DJ, Oliver E, Gilman S. Diagnostic criteria for Parkinson disease. Archives of neurology. 1999;56(1):33-9.
31. Emre M, Aarsland D, Brown R, Burn DJ, Duyckaerts C, Mizuno Y, et al. Clinical diagnostic criteria for dementia associated with Parkinson's disease. Movment Disorders. 2007;22(12):1689-707; quiz 837.
32. Power JD, Barnes KA, Snyder AZ, Schlaggar BL, Petersen SE. Spurious but systematic correlations in functional connectivity MRI networks arise from subject motion. Neuroimage. 2012;59(3):2142-54.
33. Fahn S, Elton R, editors. Members of the UPDRS development committee: The unified Parkison disease rating scale. Florham Park, NJ.: Macmillan Health Care Information; 1987.
34. Folstein MF, Folstein SE, McHugh PR. “Mini-mental state”: a practical method for grading the cognitive state of patients for the clinician. Journal of psychiatric research. 1975;12(3):189-98.
35. Podsiadlo D, Richardson S. The timed "Up & Go": a test of basic functional mobility for frail elderly persons. Journal of the American Geriatrics Society. 1991;39(2):142-8.
36. Palmqvist S, Minthon L, Wattmo C, Londos E, Hansson O. A Quick Test of cognitive speed is sensitive in detecting early treatment response in Alzheimer's disease. Alzheimer's research & therapy. 2010;2(5):29.
37. Tombaugh TN, Kozak J, Rees L. Normative data stratified by age and education for two measures of verbal fluency: FAS and animal naming. Archives of Clinical Neuropsychology. 1999;14(2):167-77.
38. Power BD, Wilkes FA, Hunter-Dickson M, van Westen D, Santillo AF, Walterfang M, et al. Validation of a protocol for manual segmentation of the thalamus on magnetic resonance imaging scans. Psychiatry Research: Neuroimaging. 2015;232(1):98-105.
39. Jenkinson M, Beckmann CF, Behrens TEJ, Woolrich MW, Smith SM. FSL. Neuroimage. 2012;62(2):782-90.
40. Jenkinson M, Bannister P, Brady M, Smith S. Improved optimization for the robust and accurate linear registration and motion correction of brain images. Neuroimage. 2002;17(2):825-41.
41. Smith SM. Fast robust automated brain extraction. Human brain mapping. 2002;17(3):143-55.
42. Woolrich MW, Ripley BD, Brady M, Smith SM. Temporal autocorrelation in univariate linear modeling of FMRI data. Neuroimage. 2001;14(6):1370-86.
43. Greve DN, Fischl B. Accurate and robust brain image alignment using boundary-based registration. Neuroimage. 2009;48(1):63-72.
44. Jenkinson M, Smith S. A global optimisation method for robust affine registration of brain images. Medical image analysis. 2001;5(2):143-56.
45. Andersson JLR, Jenkinson M, Smith SM. Non-linear optimisation. FMRIB technical report TR07JA1. 2007.

46. Andersson JLR, Jenkinson M, Smith SM. Non-linear optimisation, aka spatial normalisation. FMRIB technical report TR07JA2. 2007.
47. Beckmann CF, Smith SM. Probabilistic independent component analysis for functional magnetic resonance imaging. IEEE transactions on medical imaging. 2004;23(2):137-52.
48. Salimi-Khorshidi G, Douaud G, Beckmann CF, Glasser MF, Griffanti L, Smith SM. Automatic denoising of functional MRI data: combining independent component analysis and hierarchical fusion of classifiers. Neuroimage. 2014;90:449-68.
49. Behrens TE, Johansen-Berg H, Woolrich MW, Smith SM, Wheeler-Kingshott CA, Boulby PA, et al. Non-invasive mapping of connections between human thalamus and cortex using diffusion imaging. Nature Neuroscience. 2003;6(7):750-7.
50. Woolrich MW, Behrens TEJ, Beckmann CF, Jenkinson M, Smith SM. Multilevel linear modelling for FMRI group analysis using Bayesian inference. Neuroimage. 2004;21(4):1732-47.
51. Nichols TE, Holmes AP. Nonparametric permutation tests for functional neuroimaging: a primer with examples. Hum Brain Mapp. 2002;15(1):1-25.
52. Winkler AM, Ridgway GR, Webster MA, Smith SM, Nichols TE. Permutation inference for the general linear model. Neuroimage. 2014;92:381-97.
53. Smith SM, Nichols TE. Threshold-free cluster enhancement: addressing problems of smoothing, threshold dependence and localisation in cluster inference. Neuroimage. 2009;44(1):83-98.
54. Fischl B. FreeSurfer. Neuroimage. 2012;62(2):774-81.
55. Styner M, Oguz I, Xu S, Brechbuhler C, Pantazis D, Levitt JJ, et al. Framework for the Statistical Shape Analysis of Brain Structures using SPHARM-PDM. The insight journal. 2006(1071):242-50.
56. Genovese CR, Lazar NA, Nichols T. Thresholding of statistical maps in functional neuroimaging using the false discovery rate. Neuroimage. 2002;15(4):870-8.
57. Ji G-J, Hu P, Liu T-T, Li Y, Chen X, Zhu C, et al. Functional Connectivity of the Corticobasal Ganglia–Thalamocortical Network in Parkinson Disease: A Systematic Review and Meta-Analysis with Cross-Validation. Radiology. 2018;287(3):172183.
58. Yu R, Liu B, Wang L, Chen J, Liu X. Enhanced Functional Connectivity between Putamen and Supplementary Motor Area in Parkinson's Disease Patients. PLOS ONE. 2013;8(3):e59717.
59. Göttlich M, Münte TF, Heldmann M, Kasten M, Hagenah J, Krämer UM. Altered Resting State Brain Networks in Parkinson's Disease. PLOS ONE. 2013;8(10):e77336.
60. Esposito F, Tessitore A, Giordano A, De Micco R, Paccone A, Conforti R, et al. Rhythm-specific modulation of the sensorimotor network in drug-naïve patients with Parkinson's disease by levodopa. Brain. 2013;136(3):710-25.
61. Caspers J, Mathys C, Hoffstaedter F, Südmeyer M, Cieslik EC, Rubbert C, et al. Differential Functional Connectivity Alterations of Two Subdivisions within the Right dlPFC in Parkinson's Disease. Frontiers in Human Neuroscience. 2017;11:288.
62. Fornito A, Yucel M, Wood S, Stuart GW, Buchanan JA, Proffitt T, et al. Individual differences in anterior cingulate/paracingulate morphology are related to executive functions in healthy males. Cerebral cortex (New York, NY : 1991). 2004;14(4):424-31.
63. Hillary FG, Roman CA, Venkatesan U, Rajtmajer SM, Bajo R, Castellanos ND. Hyperconnectivity is a fundamental response to neurological disruption. Neuropsychology. 2015;29(1):59-75.

64. Gorges M, Muller HP, Lule D, Pinkhardt EH, Ludolph AC, Kassubek J. To rise and to fall: functional connectivity in cognitively normal and cognitively impaired patients with Parkinson's disease. Neurobiology of Aging. 2015;36(4):1727-35.
65. Helmich RC, Derikx LC, Bakker M, Scheeringa R, Bloem BR, Toni I. Spatial remapping of cortico-striatal connectivity in Parkinson's disease. Cerebral cortex. 2010;20(5):1175-86.
66. Mevel K, Chetelat G, Eustache F, Desgranges B. The default mode network in healthy aging and Alzheimer's disease. International journal of Alzheimer's disease. 2011;2011:535816.
67. Sheline YI, Raichle ME. Resting state functional connectivity in preclinical Alzheimer's disease. Biological Psychiatry. 2013;74(5):340-7.
68. Duval C, Daneault J-F, Hutchison WD, Sadikot AF. A brain network model explaining tremor in Parkinson's disease. Neurobiology of Disease. 2016;85:49-59.
69. Müller-Oehring EM, Sullivan EV, Pfefferbaum A, Huang NC, Poston KL, Bronte-Stewart HM, et al. Task-rest modulation of basal ganglia connectivity in mild to moderate Parkinson's disease. Brain imaging and behavior. 2015;9(3):619-38.
70. Owens-Walton C, Jakabek D, Li X, Wilkes FA, Walterfang M, Velakoulis D, et al. Striatal changes in Parkinson disease: An investigation of morphology, functional connectivity and their relationship to clinical symptoms. Psychiatry Research: Neuroimaging. 2018;275:5-13.
71. Ponsen MM, Stam CJ, Bosboom JLW, Berendse HW, Hillebrand A. A three dimensional anatomical view of oscillatory resting-state activity and functional connectivity in Parkinson's disease related dementia: An MEG study using atlas-based beamforming. Neuroimage: Clinical. 2013;2:95-102.
72. Guan X, Zeng Q, Guo T, Wang J, Xuan M, Gu Q, et al. Disrupted Functional Connectivity of Basal Ganglia across Tremor-Dominant and Akinetic/Rigid-Dominant Parkinson's Disease. Front Aging Neurosci. 2017;9:360.
73. Eckert T, Tang C, Eidelberg D. Assessment of the progression of Parkinson's disease: a metabolic network approach. The Lancet Neurology. 2007;6(10):926-32.
74. Szewczyk-Krolikowski K, Menke RA, Rolinski M, Duff E, Salimi-Khorshidi G, Filippini N, et al. Functional connectivity in the basal ganglia network differentiates PD patients from controls. Neurology. 2014;83(3):208-14.

Supporting Information captions

Supplementary Table S1. Correlations between functional connectivity and clinical data. All values are rounded to two decimal places. VLp/VA thalamus, clusters 1-6, MD/A thalamus clusters 7-9. Significance based on a two-tailed Pearson correlation controlling for age, sex and years of education. A correction for multiple comparisons using the Bonferroni method stipulate a *p*-value of < 0.000925 required for significance (based on performing 54 analyses). LED, levodopa equivalent dosage; UPDRS-III, Unified Parkinson's Disease Rating Scale part III; TUG, Timed Up and Go test; AQT, A quick test of cognitive speed test; AF, Animal fluency test.

744
745 **Supplementary Table S2. Correlations between thalami volumes and clinical measures: PD and**
746 **Controls.** A correction for multiple comparisons using the Bonferroni method stipulate a *p*-value of <
747 0.00625 required for significance (based on performing 8 analyses). UPDRS-III, Unified Parkinson's
748 Disease Rating Scale part III; TUG, Timed up and Go test; AQT, A Quick Test of Cognitive Speed;
749 AF, Animal Fluency test; R^2 change, variance in clinical measure score explained by unique
750 contribution of the volume of interest (multiply by 100 to find percentage); β, standardized beta
751 coefficient, indicating effect size.

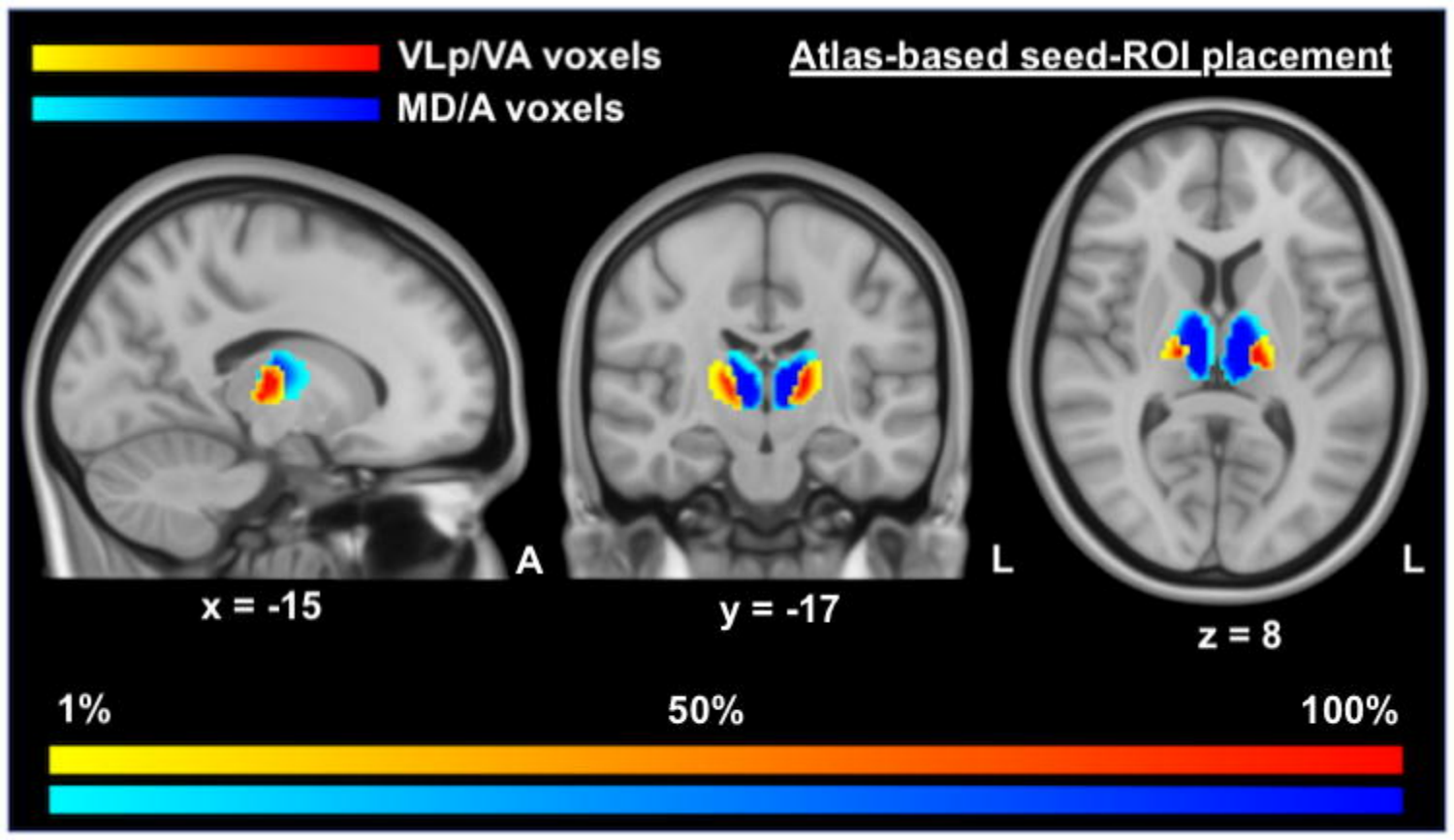
VLp/VA voxels
MD/A voxels
Atlas-based seed-ROI placement
A
L
L
x = -15
y = -17
z = 8
1%
50%
100%

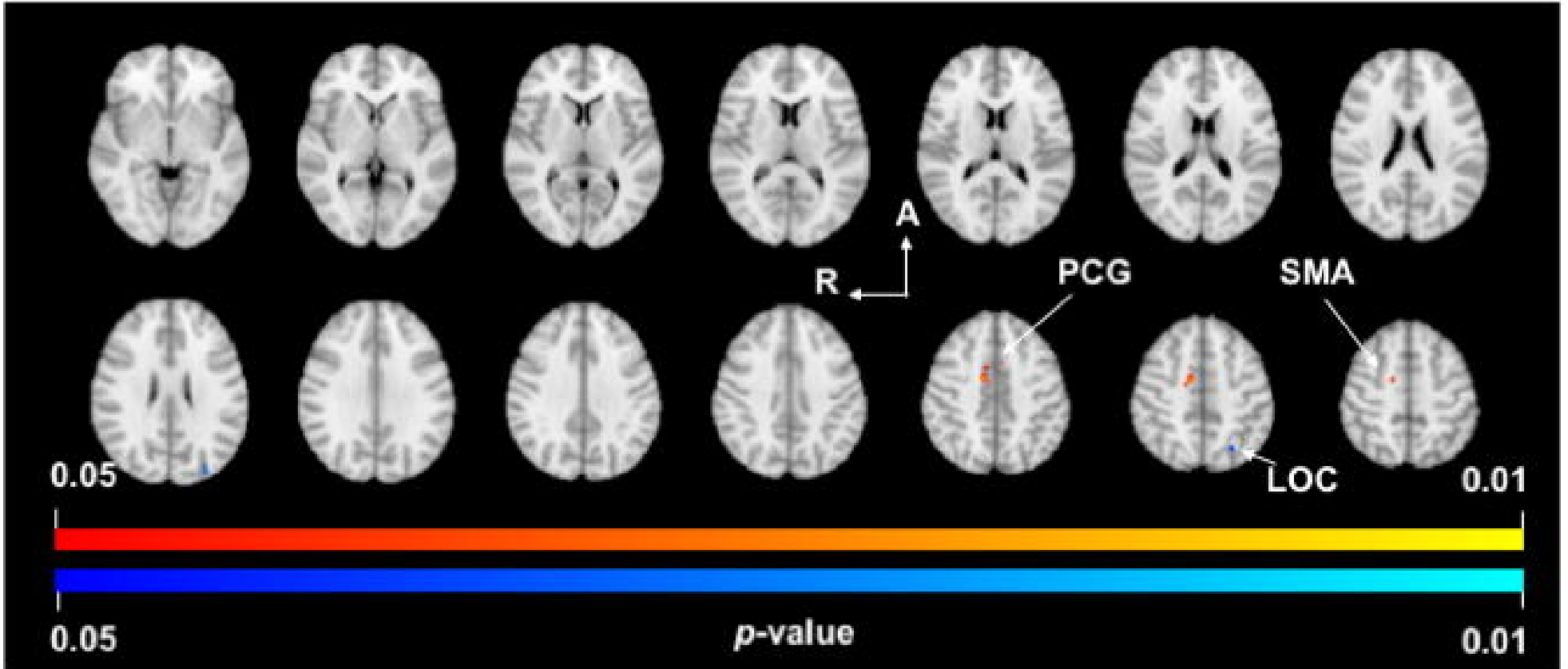
A
R
PCG
SMA
LOC
0.05
0.01
0.05
p-value
0.01

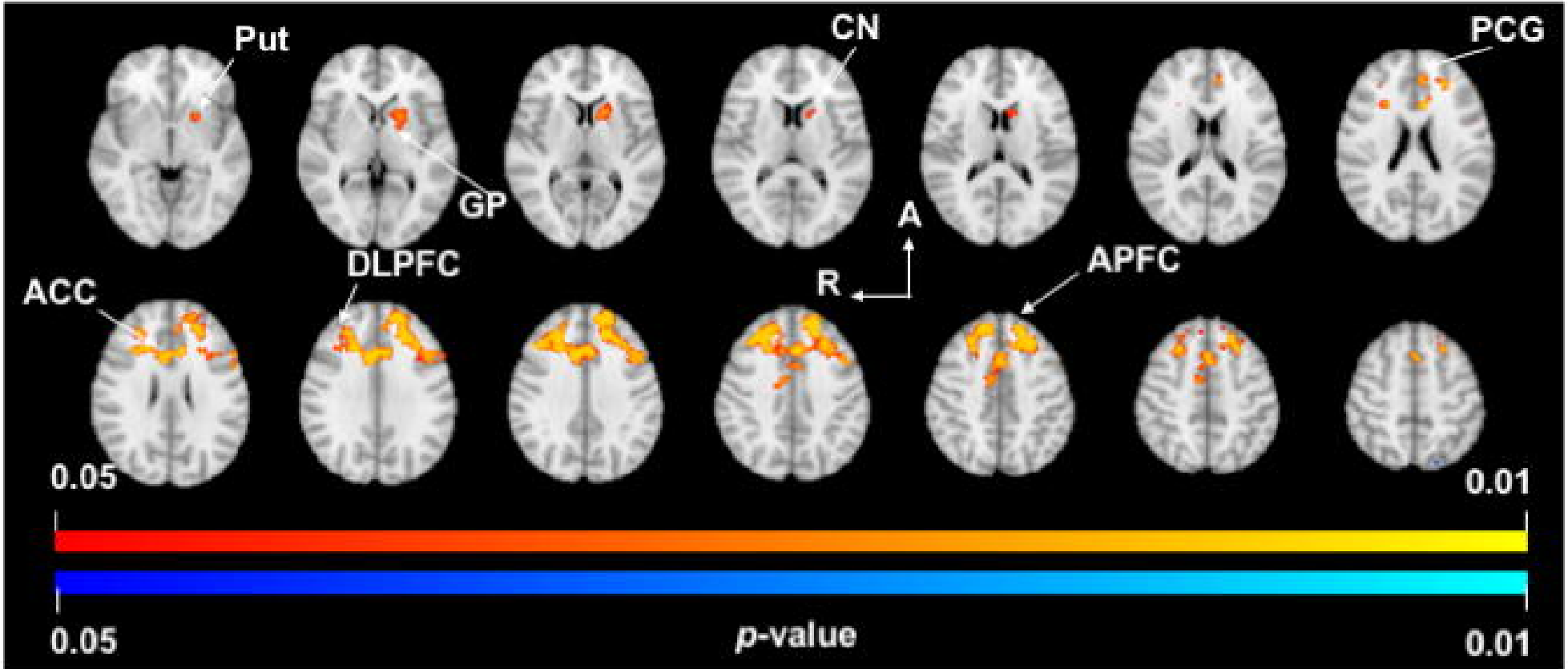
Put
CN
PCG
GP
A
R
DLPFC
APFC
ACC
0.05
0.01
0.05
p-value
0.01

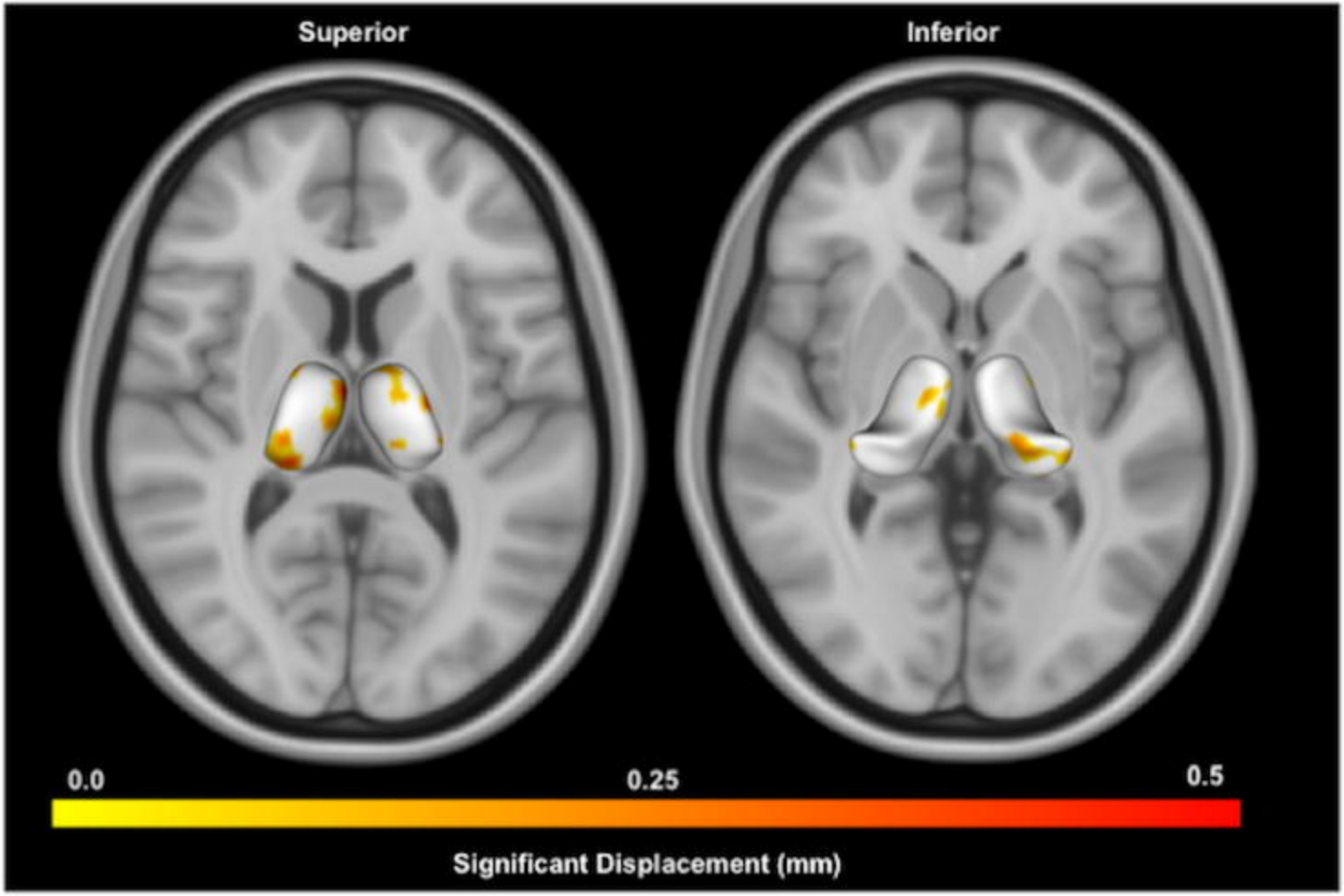
Superior
Inferior
0.0
0.25
0.5
Significant Displacement (mm)